Proceedings of the ASME 2017 Dynamic Systems and Control Conference
DSCC 2017
October 11-13, 2017, Tysons Corner, United States

DSCC2017-5236

TOPOLOGY OPTIMIZATION OF STRUCTURAL SYSTEMS CONSIDERING BOTH COMPLIANCE AND INPUT OBSERVABILITY

Yi Ren,* Houpu Yao
Mechanical and Aerospace Engineering
Arizona State University
Tempe, Arizona, 85287
Email: {yiren,hope-yao}@asu.edu

Xinfan Lin
Mechanical and Aerospace Engineering
University of California, Davis
Davis, California, 95616
Email: lxflin@ucdavis.edu

ABSTRACT

Recent advances in flexible and wireless sensors, soft materials, and additive manufacturing, have stimulated demands for developing intelligent systems that can achieve multidisciplinary objectives (e.g., mechanical strength, thermal conductivity, state and input estimation, controllability, and others). Existing studies often decouple these objectives through sub-system level design, e.g., topology and material design for mechanical and thermal properties, and filter and sensor/actuator design for observability and controllability, assuming that the sub-systems have minimal influences to each others. To investigate the validity of this assumption, we take a unique angle at studying how the topology of the system influences both structural performance (e.g., compliance under static loads) and input observability (e.g., the error in estimating the loads). We reveal a tradeoff between these two objectives and derive the Pareto frontier with respect to the topology. This preliminary result suggests the necessity of a multiobjective formulation for designing intelligent structures, when significant tradeoffs among system objectives exist.

Nomenclature

m	Input dimension
n	State dimension ($n = 2n_d$)
n_d	DOF of the finite element model
n_m	DOF of each finite element
n_x	Number of finite elements in x direction
n_y	Number of finite elements in y direction
r	Output dimension

1 Introduction

We consider the *topology* design of mechanical structures with respect to both its *compliance* under static loads and *input observability*. The former measures structural stiffness, while the latter the accuracy of estimating unknown inputs (e.g., external forces or heat sources) from potentially noisy output measurements (e.g., displacement, acceleration, and temperature). Demand grows for structures with both desired compliance (e.g., low compliance for supporting structures and high compliance for compliant mechanisms [1]) and high observability, as technologies in wireless sensing, materials, and additive manufacturing continue to advance. Such novel structures (or meta-materials) that satisfy both mechanical and control requirements have wide applications in automotive, civil engineering, robotics, soft electronics, and other engineering domains.

Existing studies typically decouple the structural design for compliance [2–4] from the sensor/filter design for input observability [5, 6]. Existing research on this issue often use the assumption of known initial system states. The input observability is hence equivalent to the invertibility of the system [5,7,8]. Some others drop this assumption and investigate the feasibility of joint state and input estimation [9, 10], rendering stricter conditions for observability. Based on the observability analysis, different methods/algorithms have been proposed to solve the input esti-

*Address all correspondence to this author.

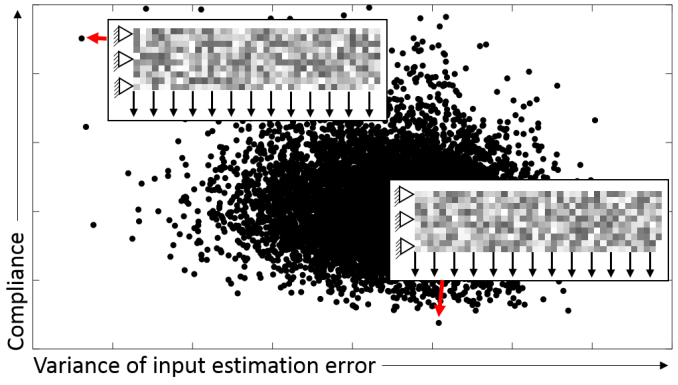

FIGURE 1. Cantilever beams with random topology (i.e., mass distributions) show tradeoff between compliance and observability. Compliance is calculated based on the static equilibrium state under the applied boundary conditions. Observability is defined as the variance of the input estimation error under output measurement noises. See Sec. 2 for more rigorous definitions of these two criteria. Insets show two sample topologies and the boundary conditions.

mation problems [11–15]. Some of the works study the estimation problem in the context of structure system dynamics [6, 16]. Recently, there have also seen efforts in sensor deployment for sensor-structure integration [17, 18]. However, the influence of structure topology on input observability is rarely investigated.

The unique contribution of this paper is thus to quantify the influence of topology design on both compliance and input observability. We show that there exists a tradeoff between these two criteria with respect to the topology (as demonstrated in Fig. 1), and formulate a compliance minimization problem with an observability constraint. We then derive the optimality conditions of the resultant problem and propose an efficient algorithm to search for topologies that satisfy these conditions. The algorithm can be extended to other problem settings, e.g., where a target compliance is to be met.

Some assumptions should be highlighted here and will be discussed in Sec. 4: We assume an elastic material and small structural deformation, under which conditions the dynamical system can be considered as linear time-invariant; the Solid Isotropic Material with Penalization (SIMP) [19] method is used to model the material modulus-density relationship (see Sec. 3); and lastly, we assume that the potential inputs will be applied to a known finite set of locations on the structure, where accelerometers are installed.

The rest of the paper is structured as follows: We first provide background knowledge in Sec. 2. In Sec. 3 we derive the optimality conditions for the constrained topology optimization problem and propose a solution strategy based on sequential linear programming. Sec. 4 analyzed the results and discussed the limitations and extensions of the proposed method. We conclude with Sec. 5.

2 Background

Due to the multidisciplinary nature of the paper, we dedicate this section to briefly introduce the background of topology optimization and input observability.

2.1 Topology optimization

Topology optimization has been widely used to accommodate mechanical [2–4, 20, 21], thermal [1, 22], electromagnetic [23, 24], acoustical [25], and other design requirements of structures. The optimization algorithm proposed in this paper is based on the SIMP method. Here the structure under design is segmented into finite elements (see insets of Fig 1), and a density value x_i is assigned to each element: A higher density corresponds to a less porous material element and higher Yong's modulus. Reducing the density to zero is equivalent to creating a hole in the structure. Thus, the set of densities $\mathbf{x} = \{x_i\}$ can be used to represent the topology of the structure and is also considered as the variables to be optimized. A common problem that SIMP solves is compliance minimization:

$$\begin{aligned} \min_{\mathbf{x}} \quad & \mathbf{d}^T \mathbf{K}(\mathbf{x}) \mathbf{d} \\ \text{subject to:} \quad & V(\mathbf{x}) \leq v, \\ & \mathbf{K}(\mathbf{x}) \mathbf{d} = \mathbf{u}, \end{aligned} \tag{1}$$

where $V(\mathbf{x})$ is the total volume; v is an upper bound on volume; $\mathbf{d} \in \mathbb{R}^{n_d \times 1}$ is the displacement of the structure under the load $\mathbf{u}$, where n_d is the degrees of freedom (DOF) of the system (i.e., the number of x- and y-coordinates of nodes from the finite element model of the structure); $\mathbf{K}(\mathbf{x})$ is the global stiffness matrix for the structure. We shall note that the global stiffness matrix is indirectly influenced by the topology $\mathbf{x}$, through the element-wise stiffness matrix $\mathbf{K}_i = \bar{\mathbf{K}}_e E(x_i)$, where the matrix $\bar{\mathbf{K}}_e$ is predefined according to the finite element type (we use first-order quadrilateral elements throughout this paper) and the nodal displacements of the element, and $E(x_i)$ is the element-wise Young's modulus defined as a function of the density x_i: $E(x_i) := \Delta E x_i^3 + E_{\text{min}}$. This cubic relationship is commonly used to help produce structures with either 1 or 0 densities through topology optimization [26]. The term E_{min} is added to provide numerical stability.

2.2 Input observability

Input observability refers to the possibility (and accuracy) of estimating the unknown input of dynamic systems, e.g., unknown forces applied to mechanical structures, from (noisy) output measurements. In the following discussion, we denote the number of state, input, and output variables as n, m, and r, respectively.

Consider a general time-invariant discrete-time system

$$\begin{aligned} \mathbf{s}_{t+1} &= \mathbf{A}\mathbf{s}_t + \mathbf{B}\mathbf{u}_t \\ \mathbf{y}_t &= \mathbf{C}\mathbf{s}_t + \mathbf{D}\mathbf{u}_t, \end{aligned} \tag{2}$$

where t denotes the time step; $\mathbf{s} \in \mathbb{R}^n$ is the state; $\mathbf{u} \in \mathbb{R}^m$ is the input; $\mathbf{y} \in \mathbb{R}^r$ is the output. $\mathbf{A} \in \mathbb{R}^{n\times n}$, $\mathbf{B} \in \mathbb{R}^{n\times m}$, $\mathbf{C} \in \mathbb{R}^{r\times n}$, and $\mathbf{D} \in \mathbb{R}^{r\times m}$ are coefficient matrices. Assume initial state $\mathbf{s}_0 = \mathbf{0}$, $\mathbf{y}_t$ can be derived by iterating Eq. (2) as

$$\mathbf{y}_t = \sum_{k=0}^{t-1} \mathbf{C}\mathbf{A}^{t-1-k}\mathbf{B}\mathbf{u}_k + \mathbf{D}\mathbf{u}_t. \tag{3}$$

In this paper, we are interested in estimating the input sequence $\mathbf{u}_{[0-t]} = [\mathbf{u}_0, \mathbf{u}_1, ..., \mathbf{u}_t]$ from the measured output sequence $\mathbf{y}_{[0-t]} = [\mathbf{u}_0, \mathbf{u}_1, ..., \mathbf{u}_t]$. The relationship between $\mathbf{u}_{[0-t]}$ and $\mathbf{y}_{[0-t]}$ can be established based on Eq. (3) as

$$\mathbf{y}_{[0-t]} = \mathbf{O}_{[0-t]}\mathbf{u}_{[0-t]}, \tag{4}$$

where

$$\mathbf{O}_{[0-t]} = \begin{bmatrix} \mathbf{D} & \mathbf{0} & \cdots & \cdots & \mathbf{0} \\ \mathbf{CB} & \mathbf{D} & \mathbf{0} & \cdots & \vdots \\ \mathbf{CAB} & \mathbf{CB} & \mathbf{D} & \ddots & \vdots \\ \vdots & \vdots & \vdots & \ddots & \mathbf{0} \\ \mathbf{CA}^{t-1}\mathbf{B} & \mathbf{CA}^{t-2}\mathbf{B} & \cdots & \cdots & \mathbf{D} \end{bmatrix}. \tag{5}$$

In order for $\mathbf{u}_{[0-t]}$ to be observable from $\mathbf{y}_{[0-t]}$, the matrix $\mathbf{O}_{[0-t]}$ needs to be of full column rank. It is noted that the dimension of $\mathbf{O}_{[0-t]}$ is $r(t+1) \times m(t+1)$. Thus a necessary condition for observability is that the number of outputs r needs to be no less than the number of inputs m. In this paper, we consider using the minimum number of sensors for input estimation, giving $m = r$. The feedthrough matrix $\mathbf{D}$ and $\mathbf{O}_{[0-t]}$ are hence both square matrices. In this case, the necessary and sufficient condition for a full-ranked $\mathbf{O}_{[0-t]}$ matrix is a full-ranked $\mathbf{D}$.

It is noted that the input observability can also be defined in other ways. For example, the L-delay input observability is defined in [5]. In the context of L-delay observability, the input sequence $\mathbf{u}_{[0-t]}$ can be estimated based on output measurements including the ones collected after the input action period $0 - t$. Therefore, the input estimation is essentially delayed by L, giving the name L-delay observability. Readers may see that the L-delay observability is weaker than the observability condition considered in this paper.

When the observability condition is satisfied, $\mathbf{u}_{[0-t]}$ can be inverted from $\mathbf{y}_{[0-t]}$ as

$$\mathbf{u}_{[0-t]} = \mathbf{O}_{[0-t]}^{-1}\mathbf{y}_{[0-t]}. \tag{6}$$

In practice, output measurements are usually contaminated by sensor noises. Assuming that the noises are identically and independently distributed among samples with zero mean and a variance of σ_y^2, the covariance matrix of input estimation is

$$\text{cov}(\hat{\mathbf{u}}_{[0-t]}) = \sigma_y^2(\mathbf{O}_{[0-t]}^T\mathbf{O}_{[0-t]})^{-1}. \tag{7}$$

The normalized covariance matrix

$$\overline{\text{cov}}(\hat{\mathbf{u}}_{[0-t]}) = \frac{\text{cov}(\hat{\mathbf{u}}_{[0-t]})}{\sigma_y^2} = (\mathbf{O}_{[0-t]}^T\mathbf{O}_{[0-t]})^{-1}, \tag{8}$$

can be used to quantify the (relative) input observability of a system.

This paper studies the influence of topology changes on the variances of input estimations. Specifically, we use the D-optimality criterion, which is the determinant of the normalized covariance matrix, $|\overline{\text{cov}}(\hat{\mathbf{u}}_{[0-t]})|$, as the measure for input observability. Since $\mathbf{O}_{[0-t]}$ is a square matrix, $|\overline{\text{cov}}(\hat{\mathbf{u}}_{[0-t]})|$ can be computed as

$$|\overline{\text{cov}}(\hat{\mathbf{u}}_{[0-t]})| = \frac{1}{|\mathbf{O}_{[0-t]}^T||\mathbf{O}_{[0-t]}|}. \tag{9}$$

Based on the block triangular structure of $\mathbf{O}_{[0-t]}$ in Eq. (5), we have

$$|\mathbf{O}_{[0-t]}| = |\mathbf{O}_{[0-t]}^T| = |\mathbf{D}|^{t+1}, \tag{10}$$

which gives

$$|\overline{\text{cov}}(\hat{\mathbf{u}}_{[0-t]})| = \frac{1}{|\mathbf{D}|^{2(t+1)}}. \tag{11}$$

It can be seen that $|\overline{\text{cov}}(\hat{\mathbf{u}}_{[0-t]})|$ decreases with increasing $|\mathbf{D}|$. Therefore, topology design for input observability can be formulated as to maximize $|\mathbf{D}|$.

3 Problem Statement

We assume that the structure is a linear time-invariant system, which is applicable when the structure undergoes elastic and small deformation. As defined in Sec. 2.1, $\mathbf{x}$ represents the topology of the structure and $\mathbf{d}$ the nodal displacement. We further define the system state as $\mathbf{s} = \begin{bmatrix} \dot{\mathbf{d}} \\ \mathbf{d} \end{bmatrix} \in \mathbb{R}^{n\times 1}$, where $n = 2n_d$. An unknown time-variant input $\mathbf{S}_u\mathbf{u}$ is imposed on this structure, where the matrix $\mathbf{S}_u \in \mathbb{R}^{n_d\times m}$ specifies the locations of m point loads and the vector $\mathbf{u} \in \mathbb{R}^{m\times 1}$ the magnitudes of these loads.

3.1 State-space equations

The time-invariant system of linear vibration

$$\mathbf{M}\ddot{\mathbf{d}} + \mathbf{K}\mathbf{d} = \mathbf{S}_u\mathbf{u}, \tag{12}$$

has the following continuous-time state-space equation

$$\dot{\mathbf{s}} = \mathbf{A}\mathbf{s} + \mathbf{B}\mathbf{u}, \tag{13}$$

where $\mathbf{A} \in \mathbb{R}^{n\times n}$, $\mathbf{B} \in \mathbb{R}^{n\times m}$, and:

$$\mathbf{A} = \begin{bmatrix} \mathbf{0} & -\mathbf{M}^{-1}\mathbf{K} \\ \mathbf{I} & \mathbf{0} \end{bmatrix} \qquad \mathbf{B} = \begin{bmatrix} \mathbf{M}^{-1}\mathbf{S}_u \\ \mathbf{0} \end{bmatrix} \tag{14}$$

The corresponding discrete-time state-space equation is

$$\mathbf{s}_{t+1} = \tilde{\mathbf{A}}\mathbf{s}_t + \tilde{\mathbf{B}}\mathbf{u}_t, \tag{15}$$

where $\tilde{\mathbf{A}} = \exp(\mathbf{A}dt)$ and $\tilde{\mathbf{B}} = \mathbf{A}^{-1}(\tilde{\mathbf{A}} - \mathbf{I})\mathbf{B}$ for a time interval dt. Let observation be a linear combination of the state:

$$\mathbf{y}_t = \mathbf{S}_a\ddot{\mathbf{d}}_t + \mathbf{S}_v\dot{\mathbf{d}}_t + \mathbf{S}_d\mathbf{d}_t, \tag{16}$$

where $\mathbf{y}_t \in \mathbb{R}^{r\times 1}$; $\mathbf{S}_a$, $\mathbf{S}_v$, and $\mathbf{S}_d$ are all in $\mathbb{R}^{r\times n_d}$. Given Eq. (12), we can associate $\mathbf{y}_t$ with $\mathbf{s}_t$ and $\mathbf{u}_t$ as follows:

$$\mathbf{y}_t = \mathbf{C}\mathbf{s}_t + \mathbf{D}\mathbf{u}_t, \tag{17}$$

where $\mathbf{C} \in \mathbb{R}^{r\times n}$, $\mathbf{D} \in \mathbb{R}^{r\times m}$ and $\mathbf{C} = [\mathbf{S}_v, \mathbf{S}_d - \mathbf{S}_a\mathbf{M}^{-1}\mathbf{K}]$, $\mathbf{D} = \mathbf{S}_a\mathbf{M}^{-1}\mathbf{S}_u$. When only accelerometers are used, $\mathbf{C}$ reduces to $[\mathbf{0}, -\mathbf{S}_a\mathbf{M}^{-1}\mathbf{K}]$.

3.2 Gradient of observability

From Sec. 2.2, it is seen that reducing the variances of input estimates can be done through maximizing $|\mathbf{D}|$[1]. The gradient $\nabla_{\mathbf{x}}|\mathbf{D}|$ has an analytical form:

$$\begin{aligned} \frac{\partial|\mathbf{D}|}{\partial x_i} &= \frac{\partial|\mathbf{S}_a\mathbf{M}^{-1}\mathbf{S}_u|}{\partial x_i} \\ &= Tr\left(\frac{\partial|\mathbf{S}_a\mathbf{M}^{-1}\mathbf{S}_u|}{\partial\mathbf{M}^{-1}}\left(\frac{\partial\mathbf{M}^{-1}}{\partial x_i}\right)^T\right) \\ &= Tr\left(|\mathbf{S}_a\mathbf{M}^{-1}\mathbf{S}_u|\mathbf{M}^T\left(\frac{\partial\mathbf{M}^{-1}}{\partial x_i}\right)^T\right). \end{aligned} \tag{18}$$

The following background knowledge is necessary for the derivation of the "inverse-mass gradient" $\frac{\partial\mathbf{M}^{-1}}{\partial x_i}$. First, denote $\mathcal{V} : \mathbb{R}^{n\times m} \to \mathbb{R}^{nm\times 1}$ as the vectorization operation that stacks columns of a matrix vertically, and $\mathcal{V}^{-1}$ as its inverse operation. The mass matrix $\mathbf{M}$ is a function of the topology $\mathbf{x}$:

$$\mathcal{V}(\mathbf{M}) = \mathbf{G}\mathcal{V}\left(\mathcal{V}(\bar{\mathbf{M}}_e)(\Delta M\mathbf{x}^T + M_{\text{min}})\right), \tag{19}$$

where $\mathbf{G} \in \mathbb{R}^{n_d^2\times n_m^2 n_x n_y}$ is a binary matrix representing the assembly of global matrices from element-wise ones. n_x and n_y are the number of elements in each dimension, and n_m is the number of unknown parameters in each finite element (e.g., $n_m = 8$ for first-order quadrilateral elements as shown in the insets of Fig. 1). M_{min} and ΔM are the minimal mass of an element and the range of element mass, respectively; $\bar{\mathbf{M}}_e$ is a n_m-by-n_m element-wise mass matrix with fixed values for a given finite element type. Note that

$$\frac{\partial\mathbf{M}^{-1}}{\partial x_i} = -\mathbf{M}^{-1}\frac{\partial\mathbf{M}}{\partial x_i}\mathbf{M}^{-1}, \tag{20}$$

we reach the following:

$$\frac{\partial\mathbf{M}^{-1}}{\partial x_i} = -\mathbf{M}^{-1}\mathcal{V}^{-1}\left(\mathbf{G}\begin{bmatrix}\Delta M\mathcal{V}(\mathbf{M}_e)\\ \mathbf{0}\end{bmatrix}\right)\mathbf{M}^{-1}. \tag{21}$$

The gradient for observability $\nabla_{\mathbf{x}}|\mathbf{D}|$ can be calculated using Eq. (18) and Eq. (21).

3.3 Compliance minimization with the observability constraint

We solve the following problem to minimize the average compliance under a distribution of static inputs, $\mathbf{u} \sim p(\mathbf{u})$, with a constraint on observability:

$$\begin{aligned} \min_{\mathbf{x}}\ & \mathbb{E}_{\mathbf{u}\sim p(\mathbf{u})}\left[\mathbf{d}^T\mathbf{K}\mathbf{d}\right] \\ \text{subject to: } & \mathbf{K}\mathbf{d} = \mathbf{u} \\ & |\mathbf{D}| \geq \epsilon \\ & \mathbf{1}^T\mathbf{x} = v, \end{aligned} \tag{22}$$

where $\mathbf{d}$ is the *static* displacement under $\mathbf{u}$, ϵ is the lower bound on observability, and v is the volume fraction specified by the designer. The optimality conditions can be derived as

$$\begin{aligned} &\mathbb{E}_{\mathbf{u}\sim p(\mathbf{u})}\left[-\mathbf{d}^T\frac{\partial\mathbf{K}}{\partial\mathbf{x}}\mathbf{d}\right] + \lambda\mathbf{1}^T - \mu\nabla_{\mathbf{x}}|\mathbf{D}| = 0 \\ &\mathbf{1}^T\mathbf{x} = v,\ \mu \geq 0, \end{aligned} \tag{23}$$

where λ and μ are the Lagrangian multipliers. We propose a sequential linear programming approach in Alg. 1 to solve Eq. (23).

The nested linear programming problem from Alg. 1 finds a search direction that reduces the compliance, while satisfying the volume fraction constraint and density bounds. Due to the nonlinearity of $|\mathbf{D}|$ with respect to $\mathbf{x}$, a line search procedure is incorporated to ensure the feasibility of intermediate solutions with regard to the observability constraint. The initial guess of the algorithm is defined as the one that maximizes $|\mathbf{D}|$. This design is found by a separate search using $-\nabla_{\mathbf{x}}|\mathbf{D}|$ as the search direction. To handle the load distribution, the gradient $\nabla_{\mathbf{x}}c(\mathbf{x})$ is approximated using a set of inputs drawn from $p(\mathbf{u}_s)$ prior to the execution of the algorithm. In addition, artificial checkerboard pattern in topologies [27] is prevented by smoothing the gradient in each iteration. Lastly, the algorithm terminates when the maximal change in the element-wise density from the proceeding iteration is less than $\varepsilon = 10^{-3}$ or after 200 iterations.

[1] Alternatively, one could maximize the trace of $\mathbf{D}^T\mathbf{D}$ (T-optimal) or the minimal eigenvalue of $\mathbf{D}^T\mathbf{D}$ (E-optimal)

Algorithm 1 Compliance minimization with constrained observability

Input: Initial topology $\mathbf{x}_0$ such that $\mathbf{1}^T\mathbf{x}_0 = v$, $p(\mathbf{u}_s)$, $\mathbf{G}$, ϵ, v, element-wise stiffness matrix $\mathbf{K}_e$ and mass matrix $\mathbf{M}_e$, convergence tolerance ε
Output: Optimal topology $\mathbf{x}^*$
$\delta\mathbf{x} = 1$, $\mathbf{x} = \mathbf{x}_0$
while $\delta\mathbf{x} > \varepsilon$ **do**
  calculate $\nabla_{\mathbf{x}} c(\mathbf{x}) = \mathbb{E}_{\mathbf{u}\sim p(\mathbf{u})}\left[-\mathbf{d}^T \frac{\partial \mathbf{K}}{\partial \mathbf{x}} \mathbf{d}\right]$
  if $|\mathbf{D}| < \epsilon$ **then**
    calculate $\nabla_{\mathbf{x}}|\mathbf{D}|$ according to Eq. (18) and Eq. (21)
  else
    set $\nabla_{\mathbf{x}}|\mathbf{D}| = \mathbf{0}$
  derive search direction $\mathbf{g}$ through LP:

$$\begin{aligned} &\min_{\mathbf{g}} \nabla_{\mathbf{x}} c(\mathbf{x})\mathbf{g} \\ &\text{subject to: } \nabla_{\mathbf{x}}|\mathbf{D}|\mathbf{g} \geq \epsilon - |\mathbf{D}| \\ &\mathbf{1}^T\mathbf{g} = 0, -\mathbf{x} \leq \mathbf{g} \leq \mathbf{1} - \mathbf{x} \end{aligned} \tag{24}$$

  set $\alpha = 0.1$
  while $|\mathbf{D}|_{\mathbf{x}+\alpha\mathbf{g}} < \epsilon$ **do**
    $\alpha = \alpha/2$
  $\mathbf{x} = \mathbf{x} + \alpha\mathbf{g}$
  $\delta\mathbf{x} = \alpha|\mathbf{g}|$

4 Results and Discussion

We apply Alg. 1 to identify Pareto optimal topologies under two sets of boundary conditions and loads, and demonstrate in each case the tradeoff between structure compliance and input observability. The element-wise Young's Modulus mass has parameters $\Delta E = \Delta M = 1$ and $E_{\min} = M_{\min} = 10^{-9}$. The Poisson's ratio is set to 0.3. The number of elements in the example is $n_x \times n_y = 80 \times 20$. The target volume fraction is set to 30% of the maximum.

Case 1 The first case considers a beam with a deterministic input distribution at its bottom (along the horizontal direction) and fixed nodes along its left edge (in both directions). See Fig. 2c. We solve a series of problems in the form of Eq. (22) with $\ln(\epsilon) \in [51, 122]$. This range is set by examining the limits of $|\mathbf{D}|$ that can be achieved by the structure to show a full spectrum of structures from high compliance/low variances in estimation error to low compliance/high variances. From Pareto-optimal solutions (as illustrated in Fig. 2b), we pick the two extremes and compare their compliance and input observability in Fig. 2c, 2d. The sample means and sample standard deviations of input estimation errors are calculated from 1000 independent simulations with normally distributed output noise. The results are verified by the theoretical standard deviations of input estimation (diag $\left((\mathbf{O}_t^T\mathbf{O}_t)^{-0.5}\right)$).

Case 2 The second case considers the same beam with a point load where the load direction is drawn from a uniform distribution in $[0, \pi]$. Both ends of the beam are fixed. See Fig. 3c. We observe similar tradeoff between input observability and compliance as in Case 1. Note that the values of $-\log(|\mathbf{D}|)$ are of a different scale from Case 1. This is because only 2 sensors, rather than 80, are considered in this case, leading to a much smaller size of $\mathbf{D}$.

4.1 Discussion

We discuss several key limitations of the proposed problem setting and their potential solutions.

Model deficiency First, we assumed that a finite number of input locations (and directions) are known a priori, and accelerometers can be deployed to all these locations on the structure. Preliminary results show that the choice of sensor locations has a significant effect on estimation error, yet for computational tractability, we decoupled sensor deployment from topology design in this paper. It is also worth noting that the embedding of sensors may degrade the strength of the structure. Such degradation is currently neglected during the design for compliance.

Affordable sensing One significant limitation of the current problem setting is that the number of sensors has to be no less than the number of inputs. While this constraint is conveniently assumed in existing literature, see for example [12, 28], it could lead to unaffordable or infeasible implementations when a large number of potential input locations exist on complicated topologies.

This issue can be addressed in two general ways. The first solution is to identify or assume an application-dependent pattern for the input distribution. For example, loads on a bridge may vary in magnitude while share spatial and temporal patterns. Such patterns can be captured by prior knowledge and incorporated into input estimation through regularization. This method may effectively reduce the dimension of inputs to the number of parameters of the input patterns, the estimation of which may require fewer sensors.

Alternatively, we can replace the definition of input observability considered in this paper with L-delay input observability. The latter allows a delay in the estimation, and does not necessarily require that the number of outputs be no less than the number of inputs. More concretely, in the context of L-delay input estimation, the input can be estimated using measurements made over L extra steps after the input action period $0 - t$. For example, for any given $\mathbf{u}_{[0-t]}$, an augmented input sequence can be defined as $\mathbf{u}_{[0-t-(t+L)]} = [\mathbf{u}_{[0-t]}, \mathbf{0}, \cdots, \mathbf{0}]$, where the inputs after time step t are all zeros. Thus, the output sequence $\mathbf{y}_{[0-t-(t+L)]}$ generated by $\mathbf{u}_{[0-t-(t+L)]}$ represents the total measurements collected for $\mathbf{u}_{[0-t]}$. The relationship between $\mathbf{u}_{[0-t]}$

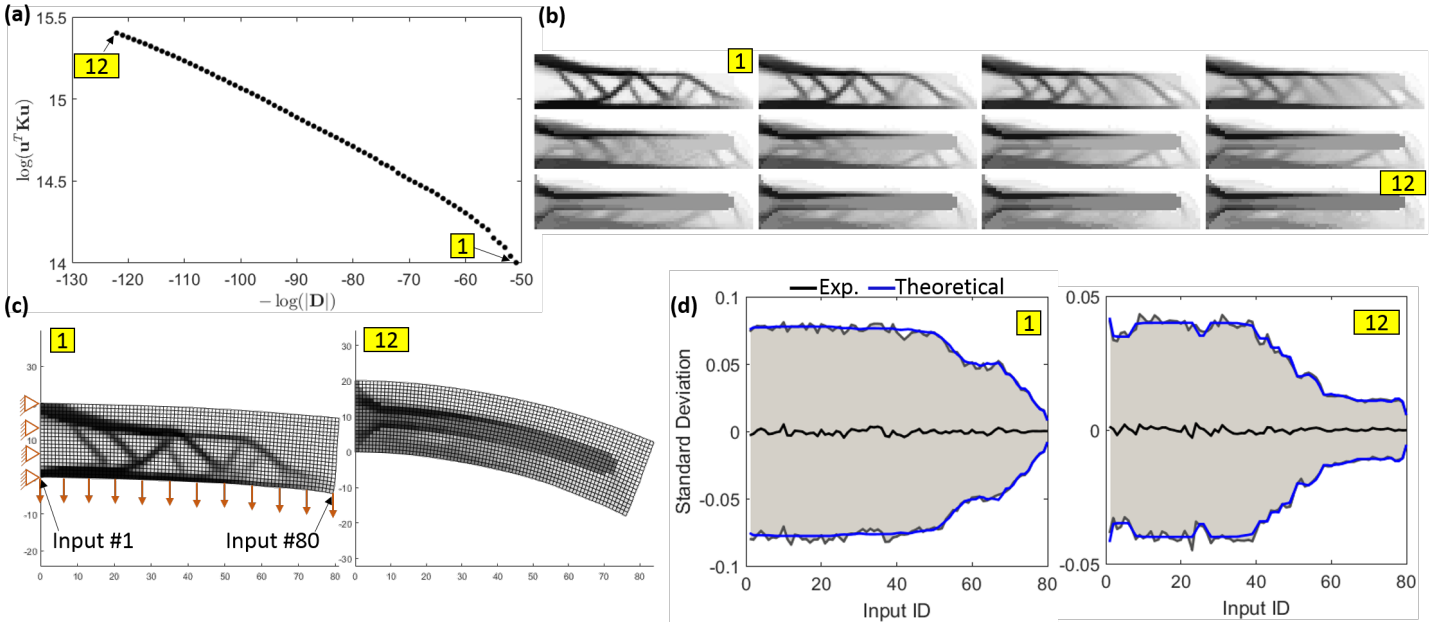

FIGURE 2. (a) Pareto-optimal topologies that trade off between input observability and compliance, (b) Visualization of topologies from (a), (c) Equilibrium states of two topologies under the given boundary conditions, (d) standard deviations of input estimation errors of the same topologies

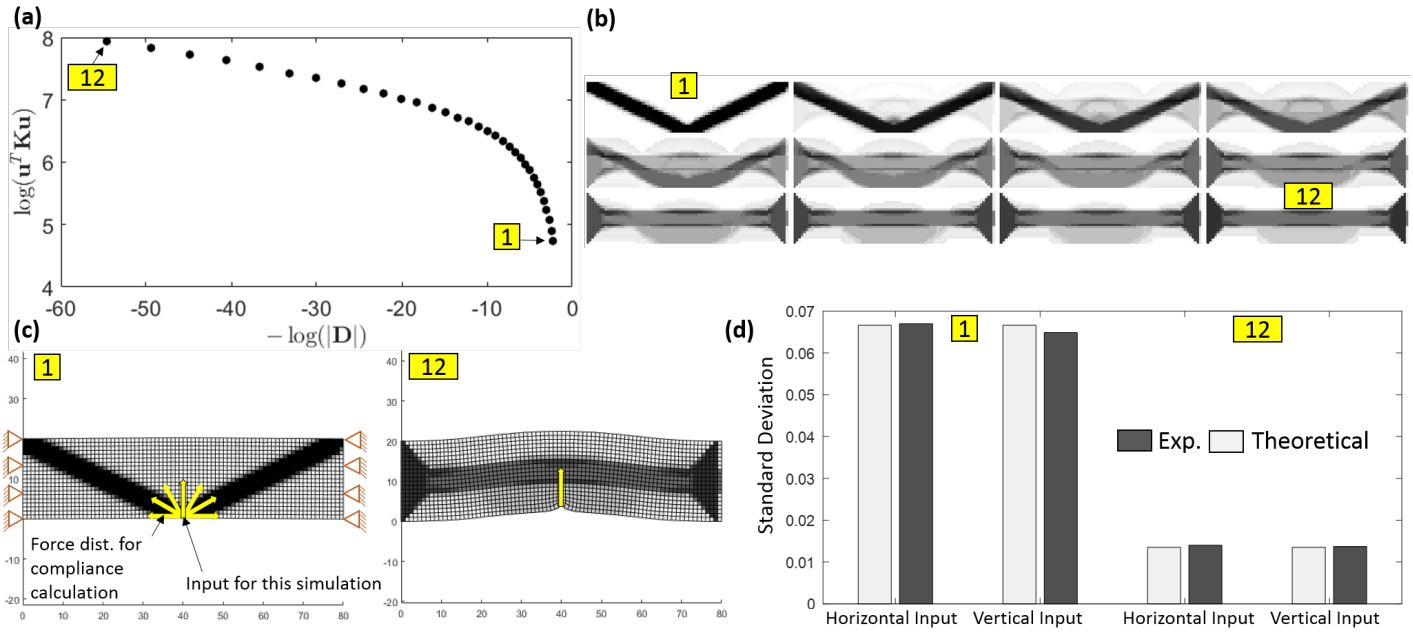

FIGURE 3. (a) Pareto-optimal topologies that trade off between input observability and compliance, (b) Visualization of topologies from (a), (c) Equilibrium states of two topologies under the given boundary conditions. The discretized input distribution is illustrated as arrows. The input used to illustrate this particular deformation is highlighted. (d) standard deviations of input estimation errors of the same topologies

and $\mathbf{y}_{[0-t-(t+L)]}$ can be established based on Eq. (3) as

$$\mathbf{y}_{[0-t-(t+L)]} = \mathbf{O}'_{[0-t-(t+L)]}\mathbf{u}_{[0-t]}, \tag{25}$$

where

$$\mathbf{O}'_{[0-t-(t+L)]} = \begin{bmatrix} \mathbf{D} & \mathbf{0} & \cdots & \cdots & \mathbf{0} \\ \mathbf{CB} & \mathbf{D} & \mathbf{0} & \cdots & \vdots \\ \mathbf{CAB} & \mathbf{CB} & \mathbf{D} & \ddots & \vdots \\ \vdots & \vdots & \vdots & \ddots & \mathbf{0} \\ \mathbf{CA}^{t-1}\mathbf{B} & \mathbf{CA}^{t-2}\mathbf{B} & \cdots & \cdots & \mathbf{D} \\ \mathbf{CA}^{t}\mathbf{B} & \mathbf{CA}^{t-1}\mathbf{B} & \cdots & \cdots & \mathbf{CB} \\ \vdots & \vdots & \vdots & \ddots & \ddots \\ \mathbf{CA}^{t+L-1}\mathbf{B} & \mathbf{CA}^{t+L-2}\mathbf{B} & \cdots & \cdots & \mathbf{CA}^{L-1}\mathbf{B} \end{bmatrix}. \tag{26}$$

The input observability can then be checked based on the column rank of $\mathbf{O}'_{[0-t-(t+L)]}$. It is noted that the dimension of $\mathbf{O}'_{[0-t-(t+L)]}$ is now $r(t+L+1) \times m(t+1)$. Therefore, as long as $r(t+L+1) \geq m(t+1)$, the number of outputs r does not need to be more than the number of inputs m in order for $\mathbf{O}'_{[0-t-(t+L)]}$ to be of full column rank.

Scalability Alg. 1 is computationally efficient as all gradients can be calculated in linear time. In addition, the calculation of $\nabla_{\mathbf{x}}|\mathbf{D}|$ can be accelerated by pre-computing the sparse tensor $\frac{\partial \mathbf{M}}{\partial \mathbf{x}}$. Nonetheless, the quadratic (in 2D) or cubic (in 3D) growth in the size of $\mathbf{x}$ with respect to the structure dimensions (or the resolution) may still cause a computational bottleneck.

5 Conclusions

We proposed a tailored sequential linear programming algorithm for structure compliance minimization with constrained input observability. The resultant Pareto-optimal topologies demonstrated the tradeoff between structure compliance and input observability. This result indicates that conventional topology designs geared towards structural requirements may suffer from high input estimation error, thus justifying the need for balancing the two criteria. By leveraging existing technology in flexible sensor networks, soft material, and additive manufacturing, the presented topology design framework will be applied to more sophisticated scenarios where nonlinear materials and multiple sensory sources are used.

REFERENCES

[1] Sigmund, O., and Torquato, S., 1997. "Design of materials with extreme thermal expansion using a three-phase topology optimization method". *Journal of the Mechanics and Physics of Solids,* ***45***(6), pp. 1037–1067.

[2] Bendsøe, M. P., and Kikuchi, N., 1988. "Generating optimal topologies in structural design using a homogenization method". *Computer methods in applied mechanics and engineering,* ***71***(2), pp. 197–224.

[3] Bendsøe, M. P., Guedes, J. M., Haber, R. B., Pedersen, P., and Taylor, J. E., 1994. "An Analytical Model to Predict Optimal Material Properties in the Context of Optimal Structural Design". *Journal of Applied Mechanics,* ***61***(4), p. 930.

[4] Buhl, T., Pedersen, C., and Sigmund, O., 2000. "Stiffness Design of Geometrically Nonlinear Structures Using Topology Optimization". *Structural and Multidisciplinary Optimization,* ***19***, pp. 93–104.

[5] Sain, M., and Massey, J., 1969. "Invertibility of linear time-invariant dynamical systems". *IEEE Transactions on automatic control,* ***14***(2), pp. 141–149.

[6] Lourens, E., Papadimitriou, C., Gillijns, S., Reynders, E., De Roeck, G., and Lombaert, G., 2012. "Joint input-response estimation for structural systems based on reduced-order models and vibration data from a limited number of sensors". *Mechanical Systems and Signal Processing,* ***29***, pp. 310–327.

[7] Silverman, L., 1969. "Inversion of multivariable linear systems". *IEEE Transactions on Automatic Control,* ***14***(3), pp. 270–276.

[8] Basile, G., and MARRQ, G., 1973. "A new characterization of some structural properties of linear systems: unknown-input observability, invertibility and functional controllability". *International Journal of Control,* ***17***(5), pp. 931–943.

[9] Hou, M., and Patton, R. J., 1998. "Input observability and input reconstruction". *Automatica,* ***34***(6), pp. 789–794.

[10] Boukhobza, T., Hamelin, F., and Martinez-Martinez, S., 2007. "State and input observability for structured linear systems: A graph-theoretic approach". *Automatica,* ***43***(7), pp. 1204–1210.

[11] Hou, M., and Muller, P., 1992. "Design of observers for linear systems with unknown inputs". *IEEE Transactions on automatic control,* ***37***(6), pp. 871–875.

[12] Gillijns, S., and De Moor, B., 2007. "Unbiased minimum-variance input and state estimation for linear discrete-time systems". *Automatica,* ***43***(1), pp. 111–116.

[13] Gillijns, S., and De Moor, B., 2007. "Unbiased minimum-variance input and state estimation for linear discrete-time systems with direct feedthrough". *Automatica,* ***43***(5), pp. 934–937.

[14] Fang, H., Shi, Y., and Yi, J., 2011. "On stable simultaneous input and state estimation for discrete-time linear systems". *International Journal of Adaptive Control and Signal Processing,* ***25***(8), pp. 671–686.

[15] Fang, H., De Callafon, R. A., and Cortés, J., 2013. "Simultaneous input and state estimation for nonlinear systems with applications to flow field estimation". *Automatica,* ***49***(9), pp. 2805–2812.

[16] Lourens, E., Reynders, E., De Roeck, G., Degrande, G., and

Lombaert, G., 2012. "An augmented kalman filter for force identification in structural dynamics". *Mechanical Systems and Signal Processing,* ***27***, pp. 446–460.

[17] Janapati, V., Kopsaftopoulos, F., Roy, S., Mueller, I., Lee, S. J., Ladpli, P., and Chang, F.-K., 2013. "Sensor network configuration effect on detection sensitivity of an acousto-ultrasound-based active shm system". In Proc. of the 9th International Workshop on Structural Health Monitoring, pp. 2147–2156.

[18] Salowitz, N., Guo, Z., Roy, S., Nardari, R., Li, Y.-H., Kim, S.-J., Kopsaftopoulos, F., and Chang, F.-K., 2013. "A vision on stretchable bio-inspired networks for intelligent structures". In Proceedings of the 9th international workshop on structural health monitoring, Vol. 1, pp. 35–44.

[19] Marck, G., Nemer, M., Harion, J.-L., Russeil, S., and Bougeard, D., 2012. "Topology Optimization Using the SIMP Method for Multiobjective Conductive Problems". *Numerical Heat Transfer Part B - Fundamentals,* ***61***, June, pp. 439–470.

[20] Van Dijk, N. P., Maute, K., Langelaar, M., and Van Keulen, F., 2013. "Level-set methods for structural topology optimization: A review". *Structural and Multidisciplinary Optimization,* ***48***(3), pp. 437–472.

[21] Wang, M., Wang, X. M., and Guo, D. M., 2003. "A level set method for structural topology optimization". *Computer Methods in Applied Mechanics and Engineering,* ***192***, pp. 227–246.

[22] Lohan, D. J., Dede, E. M., and Allison, J. T., 2016. "Topology optimization for heat conduction using generative design algorithms". *Structural and Multidisciplinary Optimization*(June), pp. 1–15.

[23] Yoo, J., Kikuchi, N., and Volakis, J. L., 2000. "Structural optimization in magnetic devices by the homogenization design method". *IEEE Transactions on Magnetics,* ***36***(3), pp. 574–580.

[24] Campelo, F., Ramírez, J. A., and Igarashi, H., 2010. "A survey of topology optimization in electromagnetics : considerations and current trends". pp. 2–47.

[25] Zhang, X., and Kang, Z., 2013. "Topology optimization of damping layers for minimizing sound radiation of shell structures". *Journal of Sound and Vibration,* ***332***(10), pp. 2500–2519.

[26] Bendsøe, M. P., and Sigmund, O., 1999. "Material interpolation schemes in topology optimization". *Archive of Applied Mechanics,* ***69***(9-10), pp. 635–654.

[27] Sigmund, O., and Petersson, J., 1998. "Numerical instabilities in topology optimization: a survey on procedures dealing with checkerboards, mesh-dependencies and local minima". *Structural and Multidisciplinary Optimization,* ***16***(1), pp. 68–75.

[28] Hsieh, C.-S., 2009. "Extension of unbiased minimum-variance input and state estimation for systems with unknown inputs". *Automatica,* ***45***(9), pp. 2149–2153.